Highly Conducting and Strongly Adhering Polypyrrole Coating Layers Deposited on Glass Substrates by a Chemical Process

F. Faverolle, A. J. Attias,* and B. Bloch

ONERA, Direction Scientifique des Matériaux 29, Av. de la Division Leclerc, B. P. 72, F 92322 Châtillon Cédex, France

P. Audebert

UFR Sciences et Techniques de Besançon, Laboratoire de Chimie Organique, F 25030 Besançon, France

C. P. Andrieux

Université de Paris 7, Laboratoire d'Electrochimie Moléculaire 2, place Jussieu, F 75251 Paris, France

Received July 2, 1997. Revised Manuscript Received December 8, 1997

To improve adhesion between polypyrrole and glass, new pyrrole-substituted organotrialkoxysilanes coupling agents are synthesized and studied. Solubility, hydrolysis, and self-condensation features in aqueous solutions are investigated by IR, ^{1}H, and ^{29}Si NMR spectroscopies. Varying the experimental conditions of pyrrole chemical polymerization on glass fibers surfaces indicates that a preliminary substrate treatment with these coupling agents and the use of a chemical vapor deposition process jointly lead to very thin (around 50 nm) polypyrrole layers with a particularly even and homogeneous aspect and adhering perfectly to glass surfaces. This last point has been plainly demonstrated by pull-out tests on conductive fibers embedded in resin and by tensile pull-off tests on silica plates. An unexpected effect of the use of specific silanes, when compared to commercial coupling agents, is an enhancement of polypyrrole conductivity (typically 150−200 S/cm), which can be related to the high regularity of the deposit.

I. Introduction

Adding special functionalities, as for instance electromagnetic shielding, to the typical mechanical properties of glass-reinforced organic composite materials is a goal that can be reached by making them conductive through some kind of modification. The main approach that has been investigated before consists of loading the resin with a conducting filler beyond the percolation threshold so that conductivity can be achieved; however, this often leads to a weakening of the mechanical properties of the composite, due to the high loading fraction currently required. A second approach would consist of the use of conducting fibers obtained by metallization. But metallization often leads to too high conductivity levels in view of the anticipated applications and, possibly, suffers from a low metal-fiber adhesion. The recently developed conducting polymers offer an alternative to the metal, provided that they can be deposited as coating layers at the surface of glass fibers. Among the wide variety of conducting polymers, polypyrrole appeared as a good candidate given its stability and its easy synthesis.

Tens of varieties of conducting polypyrroles have been described.[1] However, while electrochemistry is usually a good technique to obtain films on conducting substrates, it is more difficult to prepare, necessarily by a chemical method, very regular thin polypyrrole layers on nonconducting substrates. As for the latter, the case of glass is especially interesting, because of its many and very widespread uses.[2] Previous workers have adressed this problem, using a multiple coating deposition technique by a chemical process.[3]

When using coated fibers as reinforcement for structural composites, it is important that the inserted conducting layer does not reduce mechanical properties of the composite, because of a poor interfacial resistance. There can be no doubt that this could happen, as we ensured by preliminary tests that the adherence of the polypyrrole coatings on bare glass was practically zero. To improve the adherence of the polypyrrole coatings,

* To whom correspondence should be addressed. Tel: (+33) 1 46 73 45 72. Fax: (+33) 1 46 73 41 42. E-mail: attias@onera.fr.

(1) *Handbook of Conducting Polymers*; Skotheim T. A., Ed.; Dekker: New York, 1986.

(2) Gregory, R. V.; Kimbrell, W. C.; Kuhn, H. H. *Synth. Met.* **1989**, *28*, C823. Kuhn, H. H. *Intrinsically Conducting Polymers: An Emerging Technology* 25−34; Aldissi, M., Ed.; 1993.

(3) Nicolau, Y. F.; Nechtschein, M. *Electronic Properties of Conjugated Polymers III 91*; Kuzmany, H.; Mehring, M., Roth, S., Eds.; Springer Series in Solid State Sciences, 1989; p 461. Nicolau, Y. F.; Davied, S.; Genoud, F.; Nechtschein, M.; Travers, J. P. *Synth. Met.* **1991**, *41*−*43*, 1491.

S0897-4756(97)00466-3 CCC: $15.00
Published on Web 02/19/1998

Scheme 1

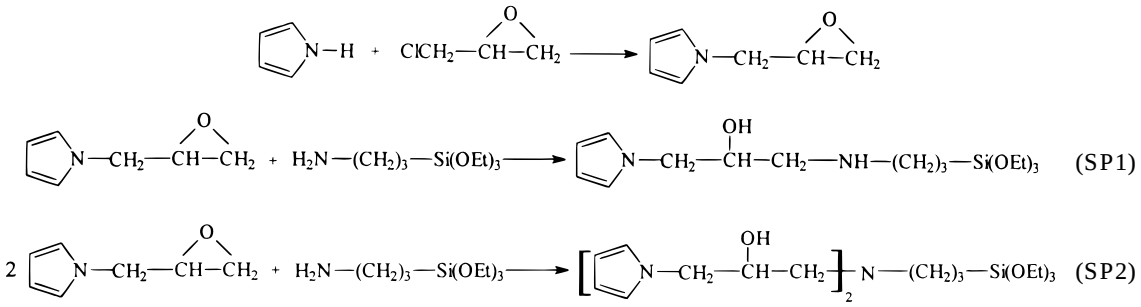

we have developed an original process based on a chemical modification of the glass fibers prior to the deposition of the conducting polymer.[4,5] This latter step can be conventionally carried out in solution or, much better, using a continuous process of polymerization from a vapor phase of pyrrole. It is worth noting that use of both these features of the process, namely the pretreatment of substrate and the vapor deposition, could be transposed to all kinds of glass or silica surfaces (fibers, plates, or fillers) and more generally inorganic materials.

The chosen method for the surface modification consists of using pyrrole-substituted organotrialkoxysilanes coupling agents. The same idea had been previously put into use for silicon wafer treatment.[6] But in the present case, we have developed several original compounds, since the choice of the surface-modifying agent has revealed itself to be especially important in relation to the properties of the resulting polypyrrole coating.[7] In addition, these new compounds were also designed in view of their ability for the most usual, simple, and straightforward technique of treatment of the glass surfaces, namely from aqueous solutions of the alkoxysilanes.

In a first part, the original synthesis of two new coupling agents, using an intermediate phase-transfer reaction, is described. Their hydrolysis features were investigated by IR and ^{1}H and ^{29}Si NMR spectroscopies in aqueous solutions in comparison with those of the well-known and currently used silane from which they are derived, viz., (3-aminopropyl)triethoxysilane. In a second part, two methods for polypyrrole coating have been described, in solution and by chemical vapor deposition, along with the physicochemical properties of the produced conducting film. The benefits of the second method are underlined. The role of the specific silanes as adhesion promoters for the polypyrrole coating is finally demonstrated by pull-out tests on coated fibers or tensile pull-off tests on plates.

II. Results

A. Silane Coupling Agent Synthesis and Processing. *A.1. Synthesis.* Organofunctional alkoxysilanes with the general formula $(RO)_nSiX_{4-n}$ where n = 1, 2, or 3 are used to modify a variety of surfaces and, more specially, glass surfaces.[8,9] Commonly named silane coupling agents, they are often used to enhance the bonding between a surface and a coating material, such as a polymer matrix. They are normally hydrolyzed in water to give silanols, before adsorption and grafting onto the surface, the silanols being the actually reacting species with the silanol and siloxane functions of the glass. For its part, the organofunctional group X is able to confer to the surface a suitable functionality, different from the original one. In our particular case, the chosen substituent, at the end of X, is a pyrrole unit, which could be anticipated to be able to fit into a growing polypyrrole chain; the hydrophilic functions introduced onto the skeleton of X could, for their part, contribute to an easy interaction and solubilization in water.

The silane previously described for polypyrrole coating of silicon wafers,[6] is *N*-(3-(trimethoxysilyl)propyl)pyrrole. The synthesis of this compound has some disadvantages, due to the use of organometallic compounds, and because 2-substituted pyrrole and disubstituted pyrrole are also obtained as byproducts.[10] In the present work, we tried to avoid such problems in synthesizing compounds, which, in addition, could be easy to use, because leading to stable aqueous solutions of silanols. The aim of a simple synthesis has been achieved by using a current commercial silane, as reactant under mild conditions with a pyrrole derivative, itself easily synthezised. With regard to our specific problems, the following pyrrole subsituted silanes, designated respectively as SP1 and SP2, have been prepared as depicted on Scheme 1.

An interesting feature lies in the preparation of *N*-glycidylpyrrole performed via a phase-transfer process. *N*-Glycidylpyrrole was previously prepared by another method,[11] but the phase-transfer reaction allows us to increase the yield to nearly quantitative by preventing the formation of 2- and 3-substituted pyrroles or polysubstituted materials as in the former way. Such use of phase-transfer or related reactions for preparing *N*-alkylated pyrroles was previously reported.[12] It has been found that *N*-alkylation of heterocyclic compounds bearing an acidic hydrogen atom attached to nitrogen can be accomplished with 18-

(4) Bloch, B.; Attias, A. J.; Ancelle, J.; Andrieux, C. P.; Audebert, P. *French Patent* 2,667,599, 1990.
(5) Attias, A. J.; Bloch, B.; Faverolle, F. *French Patent* 2,697,828, 1992.
(6) Simon, R. A.; Ricco, A. J.; Wrighton, J. *J Am. Chem. Soc.* **1982**, *104*, 2031.
(7) Faverolle, F. Thesis; University Paris 6, Paris, 1994.
(8) Plueddemann, E. P. *Silanes and Other Coupling Agents*; Mittal, K. L., Ed.; 1992; p 3.
(9) Walker, P. *Silanes and Other Coupling Agents*; Mittal, K. L., Ed.; 1992; p 21.
(10) Hobbs, C.F.; McMillan, C.K.; Papadopoulos, E. P.; Van der Werf, C. A. *J. Am. Chem. Soc.* **1962**, *84*, 43.
(11) Tanis, S. P.; Raggon, J. W. *J. Org. Chem.* **1987**, *52*, 819.
(12) Guida, W. C.; Mathre, D. J. *J. Org. Chem.* **1980**, *45*, 31721.

crown-6 employed as the catalyst, potassium *tert*-butoxide as the base, and alkyl halide as the alkylating agent. This procedure is convenient, and mild, and gives rise to exclusive *N*-substitution. Another paper describes the glycidylation of alcohols by epichlorohydrin in the presence of base in phase-transfer conditions.[13] We have adapted this reaction to the case of pyrrole, using a quaternary ammonium salt as the catalyst. Only the *N*-substituted compound is formed with a high yield. As this reaction does not proceed when the compound to be alkylated is a base, the success of this attempt can be related to the acidic, rather than basic, character of the NH group of pyrrole.

It is then possible to prepare nearly quantitatively SP1 or SP2 according to the proportion of reactants, by reaction in very mild conditions of (3-aminopropyl)-triethoxysilane (APS) with *N*-glycidylpyrrole (molar proportion 1:1 or 1:2). NMR spectra of pyrrole-substituted silanes were interpretated according to previous results on epoxy/amines resins.[14]

A.2. Hydrolysis−Condensation Process. Because organofunctional alkoxysilanes are generally applied from water or water−solvent mixtures, it is important to understand their reactions with water. In the presence of water, hydrolysis occurs to give alkoxysilanols, followed by condensation of silanols to siloxanes. Understanding the kinetics of the hydrolysis and condensation reactions for a specific silane in aqueous solution is important, because they define the lifetime of the treating solutions. The effectiveness of the silane as an adhesion promoter is influenced by the extent of condensation at the moment of the surface treatment, the presence of condensed species leading generally to poorer interfaces.

The parameters governing the solubility, the reaction kinetics, the stability, and the reactivity of silanols in solution include the nature of the organofunctional group X, the concentration of silane, the nature of the solvent, the pH of the solution, and the aging time in solution.[15]

As SP1 and SP2 silanes are new and original compounds, their solubility, hydrolysis, and condensation reactions are investigated with respect to the previous parameters. SP1 and SP2 being respectively secondary and tertiary amines, the amine class is taken into account, by comparing one silane to the other and also to APS, which is a primary amine.

A.2.a. Solubilization in Water. It is demonstrated in the literature[16−18] that the hydrolysis of APS occurs under either acid-catalyzed conditions or at natural pH without additive, i.e., under basic conditions. When no acid is added, SP1 and SP2 remain insoluble, whatever the concentration may be; with acid addition, hydrolysis and solubilization could be achieved as shown by the results reported, for different pH and silane concentrations, in Table 1. The solubility can be observed for a wide pH range. A higher degree of substitution of the amine group decreases the solubility, i.e., APS > SP1 > SP2. From a qualitative point of view, these results confirm the data concerning the influence of the organofunctional group type on the solubility and consequently on the hydrolysis process.

Table 1. Comparison of the Solubilities of APS, SP1, and SP2 for Different Silane Concentrations and pH[a]

	APS				SP1				SP2			
pH	1%	2%	5%	10%	1%	2%	5%	10%	1%	2%	5%	10%
3.1	S	S	S	S	S	S	S	E	S	S	S	E
3.5	S	S	S	S	S	S	S	E	S	S	E	E
4.5	S	S	S	E	S	S	S	E	E	E	E	E
5	S	S	E	E	E	E	E	E	E	E	E	E

[a] Status of the solution: E, emulsion; S, soluble.

Table 2. Assignments of the Infrared Bands of the Chemical Species Present during the Hydrolysis and Condensation Processes

band maximum (cm^{-1})	band assignments
silane	
1166	$\rho(CH_3)$
1103	$\nu_{as}(Si-O-C)$
1080	$\nu_s(C-O)$
958	$\nu_{as}(Si-O-CH_2)$
siloxane	
1105	$\nu_{as}(Si-O-Si)$
ethanol	
1090	$\rho(CH_3)$ and $\delta(OH)$
1045	$\nu_{as}(C-O)$
927	$\nu_{as}(Si-OH)$
870	$\nu_{as}(C-O)$
ethanol-*d*	
1092	$\rho(CH_3)$
1047	$\nu_{as}(C-O)$
930	$\nu_{as}(Si-OD)$
870	$\nu_s(C-O)$ and $\delta(OD)$

A.2.b. IR Measurements. As described in the literature,[19] the hydrolysis was at first studied by monitoring, by IR spectroscopy, the disappearance of the ethoxy group, and the amount of ethanol produced. The condensation is displayed by the formation of siloxane bonds. Due to very strong infrared absorption bands in the 3700 and 3000 cm^{-1} region and between 1850 and 1450 cm^{-1}, the spectral window of interest is narrowed between 1200 and 900 cm^{-1}. By using D_2O, it could be possible to extend the lower limit of the spectral window to 800 cm^{-1}. Despite the fact that D_2O is a more interesting solvent from this viewpoint, hydrolysis in H_2O, as the solvent used in actual practice, had still to be studied, since it has been reported[20] that the hydrolysis rate could be different in one or the other solvent.

Figure 1 shows the evolution of spectra during the hydrolysis of SP1 in H_2O and D_2O. Assignments of the infrared bands of the chemical species present during the hydrolysis−condensation process are reported in Table 2. It is obvious that the disappearance of the ethoxy can be followed by using the $\rho(CH_3)$ band at 1167 cm^{-1} and the $\nu_s(Si-O-C)$ band at 958 cm^{-1}. The formation of ethanol can be monitored by using the

(13) Mouzin, G.; Cousse, H.; Rieu, J. P.; Duflos, A. *Synthesis* **1983**, 117.
(14) Attias, A. J. Thesis; Université Paris 6: Paris, 1988. Attias, A. J.; Bloch, B.; Lauprêtre, F. *J. Polym. Sci. Part A* **1990**, *28*, 3445.
(15) Plueddemann, E. P. *Silanes Coupling Agents*; Plenum Press: New York, 1982; Chapter 1.
(16) Ishida, H. *Polym. Composites* **1984**, *5*, 101.
(17) Arkles, B.; Steinmetz, J. R.; Zazyczny, J.; Mehta, P. *Silanes and Other Coupling Agents;* Mittal, K. L. Ed.; 1992; p 91.
(18) Ishida, H.; Koenig, J. L. *Polymer* **1982**, *23*, 251.
(19) Ishida, H.; Naviroj, S.; Tripathy, S. K.; Fitzgerald, J. J.; Koenig, J. L. *J. Polym. Sci.* **1982**, *20*, 701.
(20) Lund, C. J.; Murphy, P. D.; Plat, M. V. *Silanes and Other Coupling Agents;* Mittal, K. L., Ed.; 1992; p 423. McNeil, K. J.; Di Caprio, J. A.; Walsh, D. A.; Pratt, R. F. *J. Am. Chem. Soc.* **1980**, *102*, 1859.

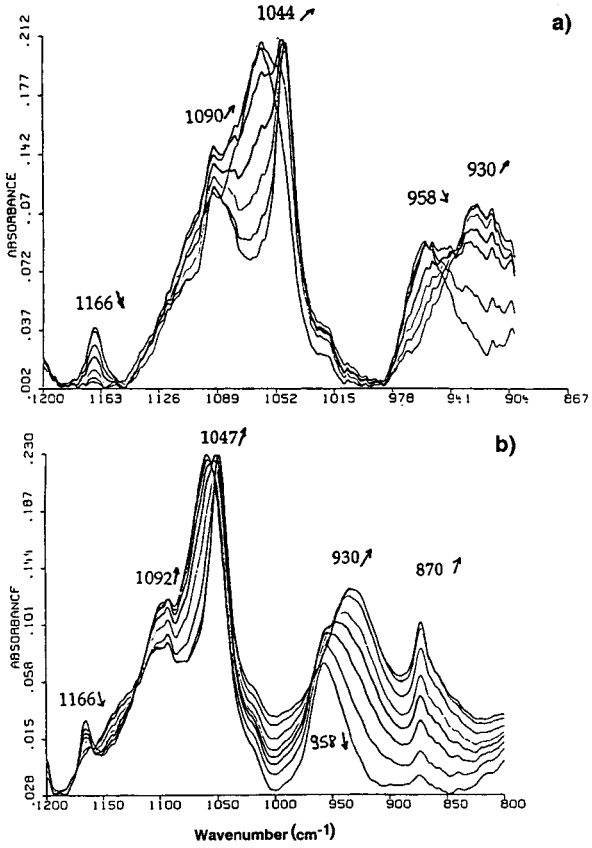

Figure 1. Evolution of IR spectra during the hydrolysis of SP1, 0.29 M in (a) H_2O; and (b) D_2O. Arrows indicate the direction of variation of the peaks.

$\rho(CH_3)$ band at 1090 cm^{-1}, the $\nu_{as}(C-O)$ band at 1045 cm^{-1}, and the $\nu_s(C-O)$ band at 870 cm^{-1}. The condensation is displayed by considering the $\nu_{as}(Si-OH)$ or $\nu_{as}(Si-OD)$ band at 927 or 930 cm^{-1} and the $\nu_{as}(Si-O-Si)$ bands between 1100 and 1000 cm^{-1}.

As shown in Figure 1a and 1b, the $\rho(CH_3)$ ethoxy band (1167 cm^{-1}) disappears, indicating complete hydrolysis of the ethoxy group, after 75 and 180 min in H_2O and D_2O solution, respectively. This analysis is confirmed by the replacement of the $\nu_s(Si-O-C)$ ethoxy band at (958 cm^{-1}) by the $\nu_{as}(Si-OH)$ or $\nu_{as}(Si-OD)$ bands (927 or 930 cm^{-1}). These results are corroborated by the investigation of bands relative to the produced ethanol. After completion of the hydrolysis, the absorbances of these latter bands do not change any longer. Concerning the condensation, the analysis is more critical due to the fact that only the $\nu_{as}(Si-OD)$ band (930 cm^{-1}) is well-defined enough to be integrated. Moreover it is impossible to discriminate the siloxanes type (degree of condensation) through the Si−O−Si band in the 1100 cm^{-1} region. Similar results have been obtained with the other silanes SP2 and APS.

From a quantitative point of view, it seems that, in H_2O, only the decrease of the silanes can be followed by integration of the $\rho(CH_3)$ ethoxy band (1167 cm^{-1}). If the solvent is D_2O, the formation of ethanol-*d* can be simultaneously followed by integrating the $\delta(OD)$ band (870 cm^{-1}). Standardization of those measurements was accomplished with solutions of varying concentrations, of silanes in CCl_4, and of ethanol-*d* in D_2O. Thus it was possible to calculate the concentrations of silane in aqueous solutions, and of silane and ethanol-*d* in

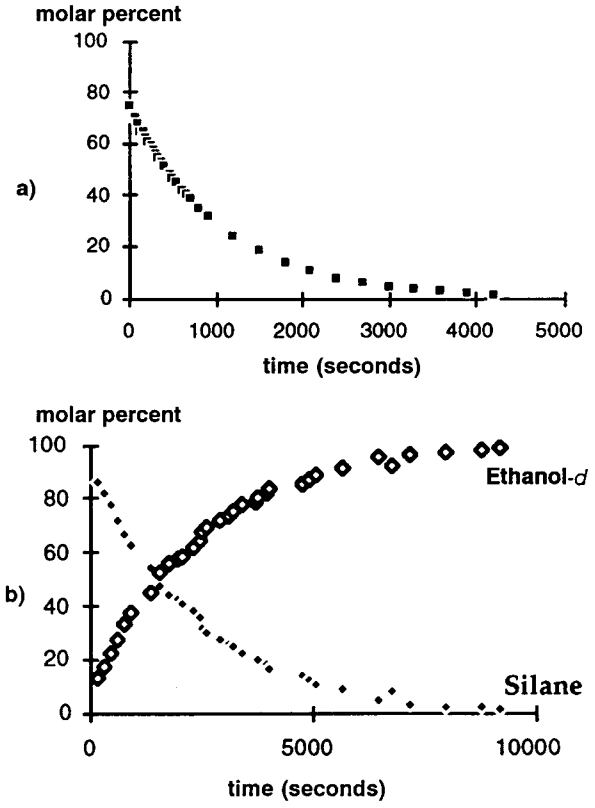

Figure 2. IR: evolution of molar percent of SP1 and ethanol versus time, during hydrolysis (a) in H_2O and (b) in D_2O (concentration of the solutions: 0.29 M).

Table 3. ^{1}H Chemical Shifts of Ethoxy Group of SP1 and of Ethanol

	^{1}H chemical shifts (ppm)	
assignment	ethoxysilane	ethanol
CH_3-CH_2-O triplet	1.07	1
CH_3-CH_2-O quadruplet	3.78	3.55

heavy water solutions. As an example Figure 2a shows the concentration decrease of silane versus time for SP1 in H_2O. In Figure 2b are reported the variations of the concentrations of residual silane and of ethanol-*d* versus time in D_2O. It is clear from the comparison of the results that the hydrolysis in D_2O is approximatively 2 times slower than in H_2O.

A.2.c. ^{1}H and ^{29}Si NMR Measurements. To confirm and extend the IR results, the ^{1}H and ^{29}Si NMR spectroscopies have been used. ^{1}H NMR is able to follow only the decrease of the alkoxy group and the formation of the corresponding alcohol,[21] and so it is applicable only to the study of the hydrolysis. On the contrary, ^{29}Si NMR is able to differentiate each silicon species, initial silanes, silanols, and siloxanes, and is thus also able to monitor the condensation of the silanols.

^{1}H chemical shifts of ethoxy group of SP1 and of ethanol are reported in Table 3. As the triplets of methyl protons of ethanol and of ethoxy are well separated enough (1.00 and 1.07 ppm respectively), it is possible to follow the formation of the former and the disappearance of the latter. The evolution of spectra of silane SP1 in H_2O versus time is displayed in Figure

(21) Blum, F. D. *Silanes and Other Coupling Agents;* Mittal, K. L., Ed.; 1992; p 181.

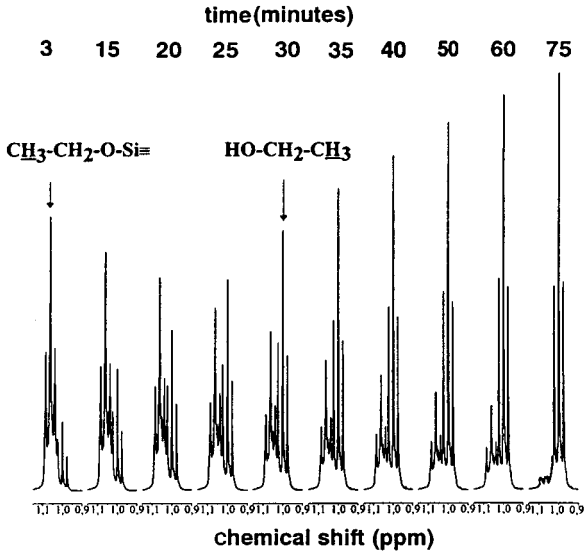

Figure 3. ^{1}H NMR: evolution of CH_3 triplets of ethoxy group and ethanol versus time during hydrolysis of SP1 (0.03 M, in H_2O).

3. They are characteristic whatever the solvent or the silane used. In the first spectrum recorded 3 min after the introduction of the silane in water (see the experimental part), the presence of triplets at 1.07 and 1.00 ppm, due to the methyl protons of ethoxy and ethanol, respectively, shows that the hydrolysis is already in progress. On the other hand, the spectrum obtained at 75 min from the first recorded spectrum shows a complete hydrolysis.

Since, as shown previously, the reactional environment has an influence on the hydrolysis of the alkoxysilane, the kinetics of the reaction has been studied. From the spectra evolutions, it is possible to qualitatively characterize the hydrolysis by following the decrease of the triplet of the ethoxy group and the increase of the triplet of ethanol. The curves in Figure 4 show that the hydrolysis is completed after 75 and 170 min (experimental time), respectively, in H_2O and D_2O.

Because of the low sensitivity of the ^{29}Si nucleus (low abundance, negative value for the gyromagnetic ratio) and the long spin−lattice relaxation time $T1$, spectra were obtained using the INEPT pulse sequence.[22] This has the advantage of producing an increase of the signal of the ^{29}Si due to polarization transfer from the ^{1}H. In our case, since the silicon does not bear any protons, we used the J^2_{SiH} coupling between silicon and protons of the CH_2 group directly bonded to Si. The chemical shifts relative to the different silanes are reported in Table 4, and the evolution versus time of ^{29}Si NMR spectra for the SP1 in H_2O is shown in Figure 5. The resonance at −45.7 ppm assigned to the nonhydrolyzed silane disappears and a peak at −42.57 ppm assigned to the complety hydrolyzed product, i.e., the silanetriol, appears. This resonance reaches a maximal value after 75 min in this case. Then it decreases and a peak at −52.16 ppm assigned to the first intermolecular condensation product appears and starts growing; this agrees well with the results given in the literature about other trialkoxysilanes.[23] Similar evolution is obtained

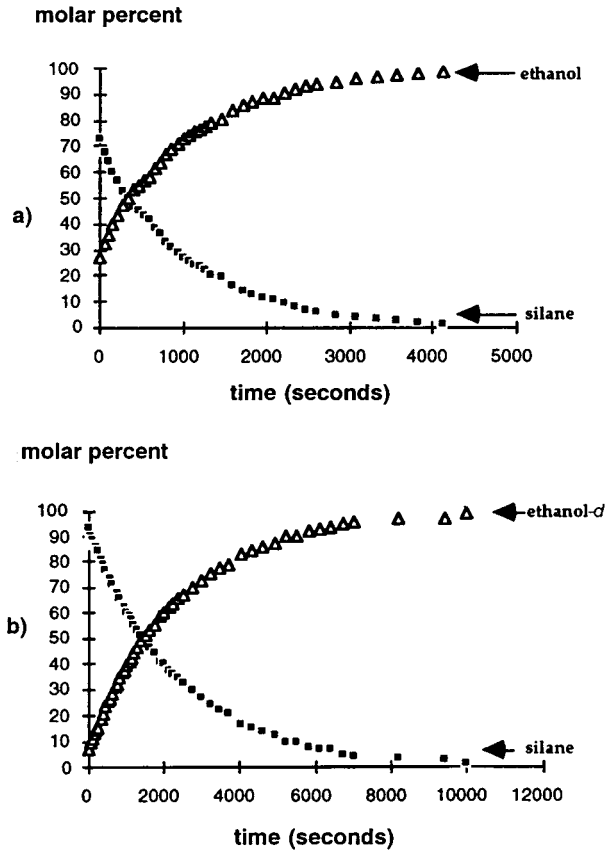

Figure 4. ^{1}H NMR: evolution of molar percent of SP1 and ethanol versus time, during hydrolysis a) in H_2O and (b) in D_2O (concentration of the solutions: 0.29 M).

Table 4. ^{29}Si Chemical Shifts of the Species Present during Hydrolysis and Condensation Processes of the Different Silanes

	^{29}Si chemical shifts (ppm)			
silane	$Si(OR)_3$	$Si(OD)_3$	$Si(OH)_3$	Si−O−Si disiloxane
SP1	−45.7	−42.6	−42.57	−52.16
SP2	−46.4	−42.82	−42.57	−52.35
APS	−46	−42.63	−42.57	−52.03

with SP1 and APS. From the spectra evolutions, it is possible to qualitatively characterize the hydrolysis by following the decrease of the Si−OR resonance and the increase of the Si−OH (Si−OD) peak.In the same way, the condensation can be monitored by the decrease of the Si−OH resonance and the increase of the Si−O−Si peak. The curves in Figure 6 show that the hydrolysis is completed after 170 mn (experimental time), in D_2O. It is worth noting that the condensation begins to proceed only after complete hydrolysis.

A.2.d. Kinetics. As shown previously, it is noticeable that the three techniques (IR, ^{1}H and ^{29}Si NMR) give results in good mutual agreement from a qualitative point of view. These results can then be used to determine the kinetic parameters for the hydrolysis of the silanes and for the ensuing condensation of the resulting silanols, with respect to several factors, such

(22) Morris, G. A.; Freeman, R. *J. Am. Chem. Soc.* **1979**, *101*, 760.
(23) Devreux, F.; Boilot, J. P.; Chaput, F.; Lecomte, A. *Phys. Rev. A* **1990**, *41*, 6901.
(24) Osterholtz, F. D.; Pohl, E. R *Silanes and Other Coupling Agents;* Mittal, K. L., Ed.; 1992; p 119. Leyden, D. E.; Atwater, J. B. *Silanes and Other Coupling Agents;* Mittal, K. L., Ed.; 1992; p 143.
(25) Smith, K. A. *J. Org. Chem.* **1986**, *51*, 3827.

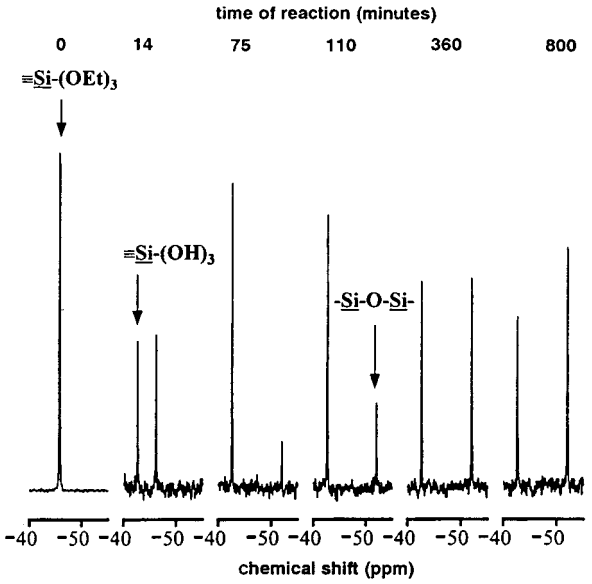

Figure 5. ^{29}Si NMR: evolution of spectra versus time (SP1, 0.03 M, in H_2O).

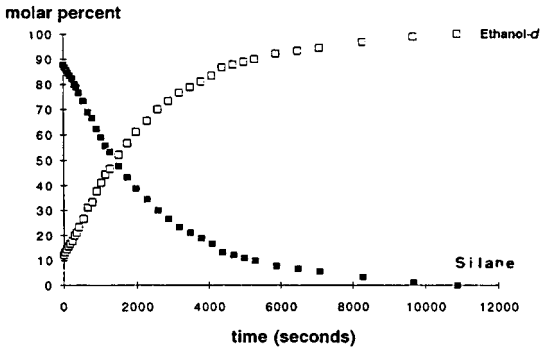

Figure 6. ^{29}Si NMR: evolution of molar percent of SP1 and ethanol versus time, during hydrolysis in D_2O (0.29 M).

as the concentration of the silane, the nature of the solvent, and the acid concentration.

Effect of the silane concentration: If we plot versus time the log of the molar percent of residual silane (or formed ethanol), determined by IR or NMR, we obtain a linear curve, indicating a first-order reaction with respect to the silane concentration, as shown in Figure 7 for SP1 in D_2O. Thus k_1, the global hydrolysis rate constant, can be calculated, and the adequate hydrolysis duration can be deduced from the extrapolation to the initial concentration of silane.[24] Moreover, $t_{1/2}$ and t_f, respectively times to half and end of reaction, have been calculated.

In Table 5 are reported results obtained by IR and NMR for two SP1 concentrations (respectively 1.5 and 10% w/w) at pH 4.5, in an acetic acid−H_2O solution. The hydrolysis follows in both cases a first-order kinetics, although the solubility behavior is different according to results reported in Table 1. The ethoxy groups are accessible for hydrolysis, though the solution, for high silane concentration, is not a true one, but rather an emulsion.

As for the condensation, by plotting the inverse of the molar percent of silanetriol versus time, we obtain a linear curve, expressing a second-order reaction with

(26) Lei, J.; Martin, R. *Synth. Met.* **1992**, *46*, 53.

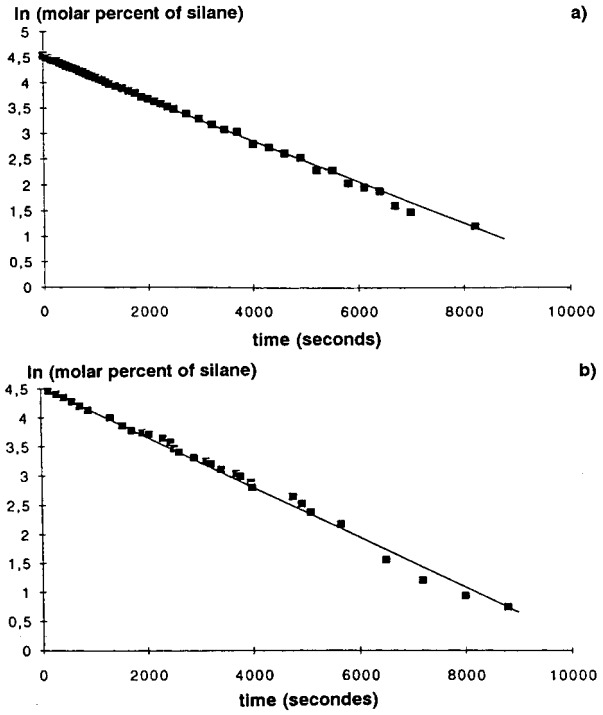

Figure 7. log of the molar percent of silane versus time for SP1 in D_2O (0.29 M). Results obtained by (a) IR and (b) NMR.

Table 5. IR and NMR Kinetics Results for Hydrolysis of SP1 (1.5% and 10% w/w in Acetic Acid−H_2O Solution)

silane SP1 mole/l	$t_{1/2}$ RMN (min)	$t_{1/2}$ FTIR (min)	t_f RMN (min)	t_f FTIR (min)	k1 RMN (10^4 s^{-1})	k1 IR (10^4 s^{-1})
0.29	12	13	75	77	9.2	8.9
0.04	13	12	74	75	9	8.5

respect to the concentration of the initial silane. Thus it is possible to have access to k_2, the condensation rate constant. Similar results are obtained with the other silanes, whatever the experimental conditions may be. For the same two concentrations of SP1 (0.04 and 0.29 M) and the same reaction medium as above, the disiloxane appears after 7 and 3.5 h, respectively. Furthermore, because the condensation begins to take place only after the end of hydrolysis, these results confirm that silanols are stable enough for use during the next 2 h.

Effect of the silane type: As shown in section A.2.a, APS is soluble whatever the pH may be, unlike SP1 and SP2, soluble only in acidic medium.

In basic solutions, the presence of the hydroxyl group in the Py−CH_2−CHOH−CH_2− substituent is not sufficient to ensure the solubilization of the substituted silanes. Moreover the silanols able to increase the solubility are not formed, suggesting that alkoxysilane groups now remain inaccessible.

In acid solutions, the solubility results from the salification of the amino group. As a result, ethoxy groups are accessible to water, and the resulting silanols increase furthermore the solubility.

In Table 6 are presented results obtained for APS, SP1, and SP2 in D_2O solution at the same molar concentration (0.214 M, which corresponds to, respectively 5, 7, and 10% w/w). Acetic acid concentration is adjusted to a pH of 4.5. It appears that the kinetic parameters are similar for the three silanes. So the

Table 6. Kinetic Parameters for Hydrolysis and Condensation of the Different Silanes at the Same Concentration (0.214 M) in D_2O (NMR results)[a]

	hydrolysis			condensation	
silane	$t_{1/2}$ (min)	t_f (min)	k_1 (10^4 s^{-1})	t_c (min)	k_2 (10^5 mol^{-1} s^{-1})
APS	25	168	4.1	187	0.625
SP1	24	150	4.56	195	1.2
SP2	25	165	4.25	240	0.95

[a] t_c: time of onset of condensation (by ^{29}Si NMR).

steric hindrance seems to have no effect on kinetics and consequently on hydrolysis mechanisms.

Concerning the acid-catalyzed condensation, APS, SP1, and SP2 behave similarly as shown by results reported in Table 6. As mentioned previously, condensation takes place only after complete hydrolysis.

Effect of the acid concentration and of the solvent: In Table 7 are reported kinetic results obtained for the hydrolysis of SP1 and SP2 in H_2O or D_2O, and for several concentrations of acetic acid: 0.33, 0.64, 1.515, 2.17 mol/L. They indicate that the rate constant k_1, for a given silane, increases with the acid concentration. In this case, according to the literature,[24,25] k_1 could be considered as a global rate constant by writing $k_1 = k[H^+]$, assuming a first-order kinetics relative to the acid concentration, k being the true rate constant. Assuming the acid concentration being in all cases higher than the silane one, the amine function of the silane is thus totally protonated, $[H^+]$ can be determined by using the following relation:

$$pH = pK_a + \log\{[A^-]/[AH]\} \quad \text{or} \quad [H^+] = K_a[AH]/[A^-]$$

where the pK_a of acetic acid is equal to 4.75, [AH] is the residual acid concentration, i.e., the difference between the initial acid and silane concentrations, and $[A^-]$ the initial silane concentration. By plotting k_1 versus $[H^+]$, a linear curve is obtained, confirming a first-order kinetics with respect to the acid concentration. Values of the rate constant k for SP1 or SP2 are respectively 11 or 12 L mol^{-1} s^{-1} in D_2O, 29 or 28 L mol^{-1} s^{-1} in H_2O.

As for the condensation following hydrolysis, Table 8 reports kinetic parameters for SP1 for two different acid concentrations in H_2O and D_2O. These results confirm again the stability of the silanols, because in all cases condensation begins only after the end of the hydrolysis. Since doubling the acid concentration increases the k_2 rate constant in the same way, this again means that this reaction is first order relative to the acid concentration.

B. Coating of the Fibers. *B.1. Elaboration of the Polypyrrole Coatings.* Two methods were explored to obtain polypyrrole layers adhering to the silanized glass fibers. In the first method, the fibers are dipped into an oxidizing aqueous solution of a ferric salt (chloride or *p*-toluenesulfonate), to which is added afterward an aqueous pyrrole solution; the fibers are then left for a certain length of time in contact with the mixture. The second method consists of dipping shortly the fibers into the oxidizing aqueous solution and then exposing them to an atmosphere saturated with pyrrole vapor at room temperature, while they are still wet. For both methods, some exploration of the relevant parameters has been performed and is detailed in the following.

In this preliminary exploration, the only tested feature was the linear resistance (resistance by unit of length) of coated fibers. In addition, through all the experimental processes tried, comparison has each time been made with a similarly polypyrrole-coated fiber but beforehand treated with a classical commercial silane, APS, which does not bear any attached pyrrolic ring, to estimate the improvement due to the specifically functionalized silanes.

B.1.a. Liquid-Phase Polymerization. Since less convincing results were obtained in this case, the number of experiments was reduced by comparison with the vapor-phase method. The results versus time and oxidant concentration are summarized in Table 9.

Conducting fibers have been obtained in every case, with a decrease of the resistance with the treatment time. It is also clear that the pretreatment of the fibers with any pyrrole-functionnalized silane, either SP1 or SP2, results in a far better conductivity of the fibers than with the standard APS. Also higher conductivities were every time achieved with SP1 rather than with SP2.

B.1.b. Vapor-Phase Polymerization. Since the results obtained in solution showed that SP1 was a better candidate to get highly conducting polypyrrole layers, this silane was the only one used throughout subsequent preparations. Table 10 shows the variation of the linear resistances versus time during which the fiber was kept in contact with the pyrrole vapor. It is clear that higher conductivities are achieved than in the solution method and in much shorter treatment times.

Table 7. Influence of pH on the Kinetic Parameters of Hydrolysis for SP1 and SP2, in H_2O or D_2O (NMR and IR results)

		hydrolysis in D_2O NMR results			IR results			hydrolysis in H_2O NMR results			IR results		
acetic acid (mol/L)	pH	$t_{1/2}$ (s)	t_f (s)	$k1$ (10^4 s^{-1})	$t_{1/2}$ (s)	t_f (s)	$k1$ (10^4 s^{-1})	$t_{1/2}$ (s)	t_f (s)	$k1$ (10^4 s^{-1})	$t_{1/2}$ (s)	t_f (s)	$k1$ (10^4 s^{-1})
						SP1 (0.29 M)							
0.33	5.2	6613	22300	1.04	4900	22800	1.4	2380	13110	3	2235	11235	2.9
0.65	4.5	1600	10210	4.1	1415	9215	4.4	731	4520	9.2	780	4600	8.9
1.515	3.9	650	3650	10.8	615	3745	11	324	2180	24	310	1920	24
2.17	3.65	450	3150	15	500	2900	15	230	1370	37	200	1150	39
						SP2 (0.214 M)							
0.33	5	2800	17700	2.45	2260	14300	3	1700	9900	4.23	1300	7400	4.9
0.65	4.2	1500	9916	4.2	1500	10300	4.1	480	3025	14	540	3060	14
1.515	3.5	620	4155	10.7	620	4300	11	250	1560	29	272	1572	27.3
2.17	3.1	350	2260	19.6	500	2400	19.4	150	920	50	136	890	54

Table 8. Kinetic Parameters of Condensation of SP1 for Two Acid Concentrations in H_2O and in D_2O[a]

	acid concentration (M)	t_f (min)	t_c (min)	$k2$ (10^5 L mol^{-1} s^{-1})
hydrolysis in H_2O	1.515	20	50	3.3
	0.65	65	125	1.6
hydrolysis in D_2O	0.65	155	205	1.5
	0.33	350	380	0.6

[a] t_f: time of completion of hydrolysis (^{1}H NMR). t_c: time of onset of condensation (^{29}Si NMR).

Table 9. Liquid-Phase Polymerization: Linear Resistance (kΩ/cm) of Fiber Tows versus Time of Polymerization in Solution for Different (Fe^{3+})/(Pyrrole) Ratios (APS, SP1, or SP2 Pretreatment)

	linear resistance (kΩ/cm)		
t (min)	SP1	SP2	APS
	(Fe^{3+})/(pyrrole) 0.1 M/0.03 M		
120	200	450	>10000
	(Fe^{3+})/(pyrrole) 0.3 M/0.03 M		
4	70	110	160
6	12	55	160
10	3	25	140
	(Fe^{3+})/(pyrrole) 0.3 M/0.03 M		
0.5	15	50	150
2	8	36	150
6	5	28	120

Table 10. Vapor-Phase Polymerization: Linear Resistance (kΩ/cm) versus Time of Polymerization (SP1 pretreatment)

t (min)	linear resistance (kΩ/cm)
0.5	7
1	3
1.5	1.2
2	1
3	0.6

C. Characterization of the Coated Fibers. *C.1. Film Appearance and Thickness.* Scanning electron microscopy experiments (SEM) have been performed on a few selected fibers; Figure 8 shows the SEM pictures of two polypyrrole-coated fibers, respectively pretreated with APS and SP1. It is clear that a much more homogeneous surface state is obtained in the case of the SP1-treated fiber. In this case, the fiber surface appears even and smooth, without observable polypyrrole grains. The coating appears highly regular and homogeneous. On the contrary, the APS-treated fiber exhibits the presence of nanometer size grains, with in addition a nonhomogeneous coverage of the fiber surface.

The film thicknesses have been indirectly determined by thermogravimetric analysis (TGA) performed in air; when the organic polypyrrole layer is burned out at 500 °C, the weight loss gives the mass percent of the polymer initially present, around 1% in most cases. Without indication on the polypyrrole layers density, we chose the commonly adopted literature value of 1.55[26] to estimate the volume percent of polypyrrole; hence, by assuming an equal thickness around each fiber, whose mean diameter is 13 μm, films thicknesses and finally intrinsic conductivities of the layers can be computed. Table 11 shows the mass percents, thicknesses, and intrinsic conductivities of the polypyrrole layers deposited on SP1-pretreated fibers according to both the oxidant concentration and the treatment time.

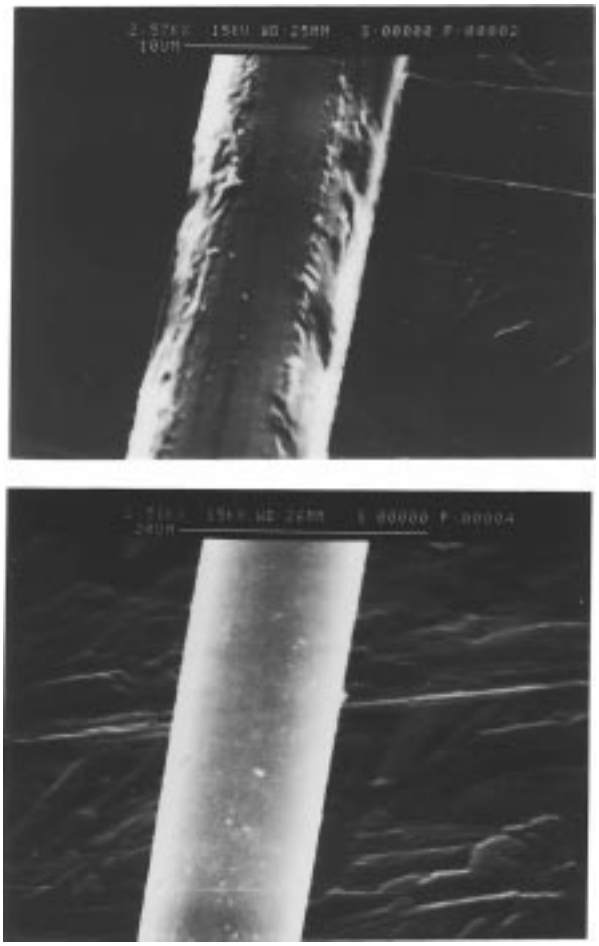

Figure 8. SEM views of the surface of polypyrrole coated fibers, pretreated with (a, top) APS and (b, bottom) SP1.

Table 11. Linear Resistance (Ω/cm), Mass Percent (in Relation to the Glass Fiber Mass), Thickness, and Intrinsic Conductivity of the Polypyrrole Layers Deposited on SP1 Pretreated Fibers According to Both the Oxidant Concentration and the Polymerization Time

t (s)	linear resistance (Ω/cm)	weight loss (%)	thickness (nm)	conductivity (Ω^{-1}/cm)
		[$Fe(Tos)_3$] (0.3 M)		
30	3500 (±300)	0.2	12	70
120	960 (±20)	0.35	20	150
240	740 (±20)	0.4	24	165
		[$Fe(Tos)_3$] (0.6 M)		
30	1100 (±200)	0.45	26	100
120	525 (±30)	0.6	35	155
240	420 (±20)	0.8	47	145

It can be seen that increasing the oxidant concentration leads to a corresponding increase in the film thickness, as could be expected, since the amount of deposited polypyrrole is directly controlled by the quantity of the oxidant solution retained inside the wet tow. The intrinsic conductivities of the polymerized layers is very high, in the 100−200 S/cm range, that is much higher than the conductivity of the conventional chemically prepared polypyrrole powders, which is most currently comprised in the 10−50 S/cm range. As reported in Table 12, this high conductivity value of our polypyrrole layers has been shown to result from the use of the specific silanization as pretreatment, other coupling agents leading to appreciably lower values. Such a behavior difference could be attributed to the continuity,

Table 12. Effect of the Nature of the Silane Pretreatment on the Electrical Properties

silane	linear resistance (Ω/cm)	thickness (nm)	conductivity (Ω^{-1}/cm)
pyrrole substituted	960	20	100
	525	35	155
nonspecific	1400	35	58
	1000	52	55

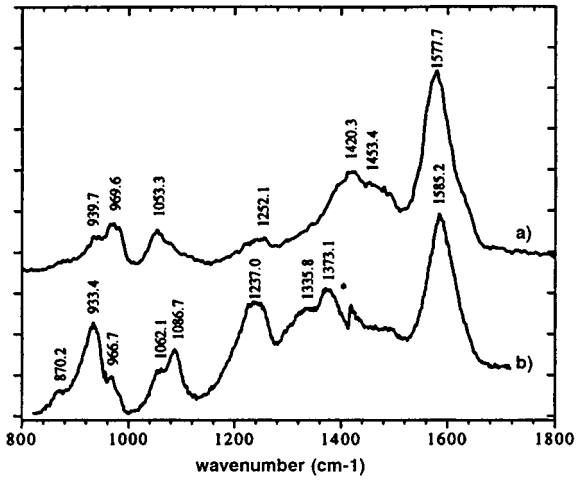

Figure 9. Micro-Raman spectra obtained from a polypyrrole-coated single fiber, for two excitation wavelengths: (a) 457.9 nm; (b) 632.8 nm.

regularity, and evenness of the layer resulting specifically from the use of pyrrole-substituted silanes.

C.2. Infrared and Micro-Raman Spectroscopy. Diffuse reflection infrared spectra have been obtained from fibers before and after polypyrrole coating. But, as in IR spectroscopy, the response is directly related to the concentration of the examined species, signals from the coating are practically completely vanishing in comparison to those coming from the glass substrate, and it would be impossible to exploit the polypyrrole lines that could remain distinguishable.

Raman spectroscopy represents a different situation, since polypyrrole is highly absorbing in the wavelength domain of the usual excitation lights, realizing thus the condition for easily obtaining resonance Raman spectra, not affected by the glass substrate. Because of the strong increase in sensitivity resulting from resonance, only the polypyrrole layer response remains detectable. Another advantage of Raman spectroscopy lies in its easy and current association with a microscopic system of examination, which makes it, in its microprobe mode, a method ideally adapted to the direct analysis of the surface of the individual fiber, without any preparation of the sample.

As an example, Figure 9 shows the resonance Raman spectra obtained from a polypyrrole-coated single fiber, with two different excitation wavelengths. These spectra show clearly the wavelength dependence of the band intensities. It is thus possible, according to Furukawa,[27] to correlate Raman bands to optical transitions, which makes Raman spectroscopy a valuable tool not only for the analysis of the deposited coatings but also for the characterization of the doping state and the related

(27) Furukawa, Y.; Tazawa, S.; Fujii, Y.; Harada, I. *Synth. Met.* **1988**, *24*, 329.

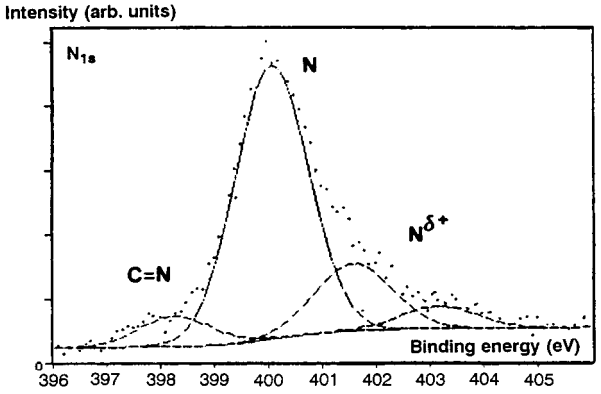

Figure 10. XPS: nitrogen 1s region: experimental data (points) and curve fits (lines).

structural distortions of the conductive polymer skeleton. The results of this application of Raman spectroscopy to the analysis of the deposited polypyrrole layers will be reported in a later paper.[28]

C.3. XPS Spectroscopy. XPS is a classical tool well adapted to the study of thin layers, allowing us to reach their chemical composition. This spectroscopy has previously been applied to the analysis of polypyrrolic materials,[29−32] because it is particularly suited for monitoring the changes in the chemical states of C and N in polypyrrole samples, mainly focusing on the N 1s and C 1s bands. Furthermore it was found that XPS provided a convenient tool for the quantitative differentiation of the various oxidation states of the pyrrolium nitrogens and so for the doping levels determination.

Actually, the interpretation of the XPS data allows us to extract with reasonable accuracy the doping level of the polypyrrole at the fibers surface, by simply determining the quantity of an element present only in the dopant. Here, the sulfur analysis can be correlated to doping toluenesulfonate. Another way consists of comparing the respective amounts of neutral and positively charged nitrogens (Figure 10).

Of course, this method supposes that we deal with sufficiently thick films, so that the bonding silane monolayer does not perturbate the analysis. The doping levels determined by both methods are in the same range and generally found between 0.25 and 0.3 as could normally be expected for polypyrrole.

D. Adherence of the Polypyrrole Layer. *D.1. Pull-Out Tests.* Demonstration of the promotion by SP1 of the adhesion of polypyrrole on glass fibers was achieved in an original way by using a pull-out test currently carried out to characterize fiber−matrix interface resistance in the field of composite materials.

D.1.1. Principle of the Pull-Out Test. Figure 11 shows a schematic view of the test. In the classical use,

(28) Vautrin, M. Thesis; Université Paris 7, Paris, 1996.
(29) Pfluger, P.; Street, G. B. *J. Phys. Colloque C3* **1983**, 609. Inganäs, O.; Erlandsson, R.; Nylander, C.; Lundström, I. *Phys. Chem. Solids* **1984**, *45*, 427.
(30) Kang, E. T.; Neoh, K. G.; Ong, Y. K.; Tan, K; L;; Tan, B. T. G. *Synth. Met.* **1990**, *39*, 169. Pigois−Landureau, E.; Nicolau, Y. F.; Delamar, M. A. *Synth. Met.* **1995**, *72*, 111.
(31) Benseddik, F.; Makhlouki, M.; Bernède, J. C.; Lefrant, S.; Pron, A *Synth. Met.* **1995**, *72*, 237.
(32) Eaves, J. G.; Munro, H. S.; Parker, D. *Polym. Commun.* **1987**, *28*, 38. Hino, S.; Iwasaki, K.; Tatematsu, H.; Matsumoto, K. *Bull. Chem. Soc. Jpn.* **1990**, *63*, 2199.

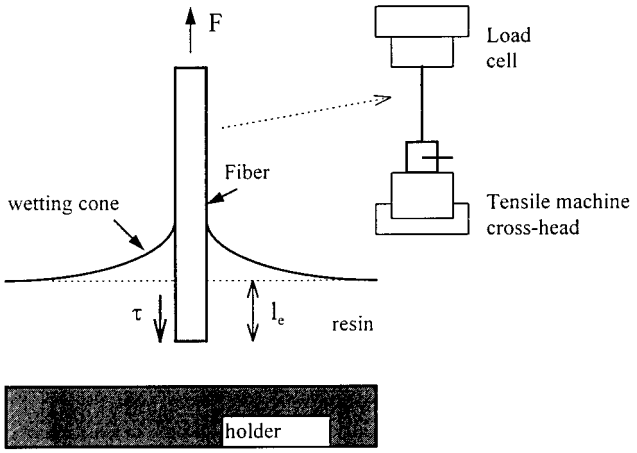

Figure 11. Scheme of the pull-out test.

a single glass fiber is embedded in a thin resin layer spread on a metallic holder. The free end of the fiber is glued to a part attached to the load cell of a tensile machine. When a force F is applied to the fiber, it generates an interfacial shear stress τ which is not uniform along the embedded length l_e but maximum near the surface of the resin. The debonding process is initiated when the latter local maximum stress attains the interfacial resistance value τ_d, for $F = F_d$. The quantity τ_d is not directly measurable, but it can be estimated from the mean value $\bar{\tau}$ of the interfacial shear stress computed from the test results:

$$\bar{\tau} = F_d/pl_e \qquad (p\text{: fiber perimeter})$$

by using eq 1, relating $\bar{\tau}$ to τ_d according to a theory established by Grezsczuk:[33]

$$\bar{\tau} = \tau_d(th\alpha l_e)/\alpha l_e \qquad (1)$$

where α is a characteristic constant of the deformation at the interface. The fit of theoretical curve given by eq 1 is carried out on experimental values of $\bar{\tau}$, obtained by varying the embedded length. This length is measured by scanning electron microscopy (SEM) or optical microscopy, after debonding.

In fact in our particular case the polypyrrole layer fills an intermediate position between glass and resin, creating two new interfaces, and it becomes important to identify which interface will be ruptured: glass−polypyrrole or polypyrrole−matrix. The estimated τ_d values will characterize this ruptured interface.

D.1.2. Results. Figure 12 shows experimental results and fits, and Table 13 gives τ_d and α values, the silanes used being respectively APS and SP1.

APS pretreatment: Figure 13a is a SEM micrograph of the embedded surface of a pulled-out glass fiber when it is treated with a nonspecific silane (such as APS). The surface appears smooth and lightened by an electrostatic charging effect. These observations make evident the fact that the surface is no longer conductive and that, therefore, the polypyrrole layer remaining bonded to the resin has been separated from the fiber. The marks of the wetting cone are not visible. This ex-

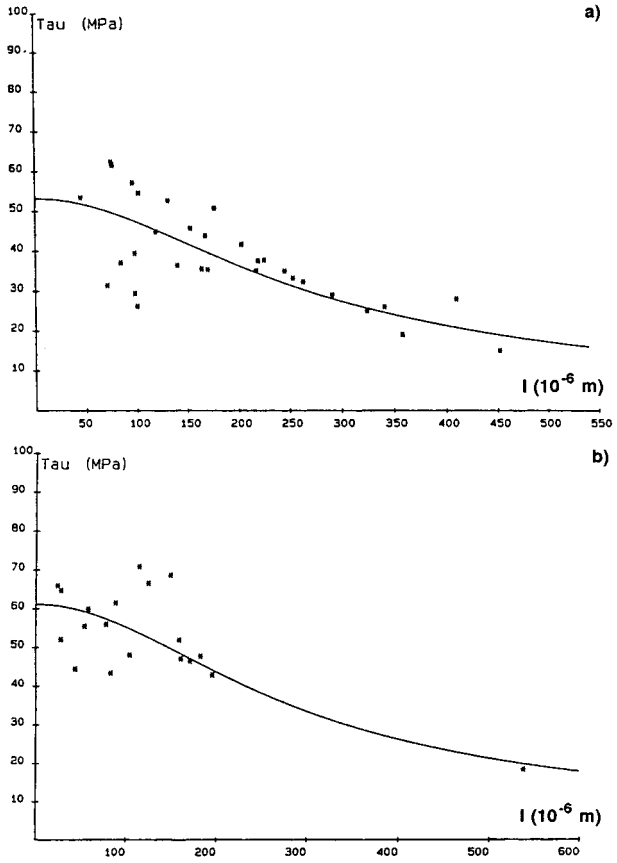

Figure 12. Pull-out test: evolution of τ (experimental data (points) and curve fits) versus the embedded length, for polypyrrole-coated fibers pretreated with (a) APS and (b) SP1.

Table 13. Results of the Pull-Out Test for APS and SP1 Pretreatments

silane	τ_d (MPa)	α (m^{-1})
APS	50	6160
SP1	65	5720

presses a true interfacial decohesion.[34] These two facts mean that the debonding takes place at the silanized glass fiber−polypyrrole interface.

This conclusion is confirmed, from a quantitative point of view, by the results deduced from the pull-out tests. The value of τ_d is equal to 50 MPa, expressing a lower interfacial adhesion compared to typical values close to 65 MPa in the case of a classical silanized glass fiber−epoxy matrix interface.[34]

From all these results it can be deduced that the adhesion of polypyrrole coating on APS-pretreated glass fiber is moderate and less than that of the polypyrrole−matrix interface. Similar results are obtained with other silanes, i.e., MPS and GPS.

Pretreatment with SP1 silane: When SP1 is used as silane, for embedding depth higher than 200 μm, it is almost impossible to pull-out the embedded length before breaking (Figure 12b). On the contrary, APS-treated fibers are easily pulled out for embedded lengths in the range 200−600 μm (Figure 12a).

The extracted surface examined by SEM does not appear modified (Figure 13b), compared to the free part of the fiber, apparently remaining conductive. This

(33) Greszczuk, L. B. *Interfaces in Composites ASTM STP 452, American Society for Testing and Materials*, 1969; p 42.

(34) Feillard, P.; Rouby, D.; Desarmot, G.; Favre, J. P. *Mater. Sci. Eng.* **1994**, *A188*, 159.

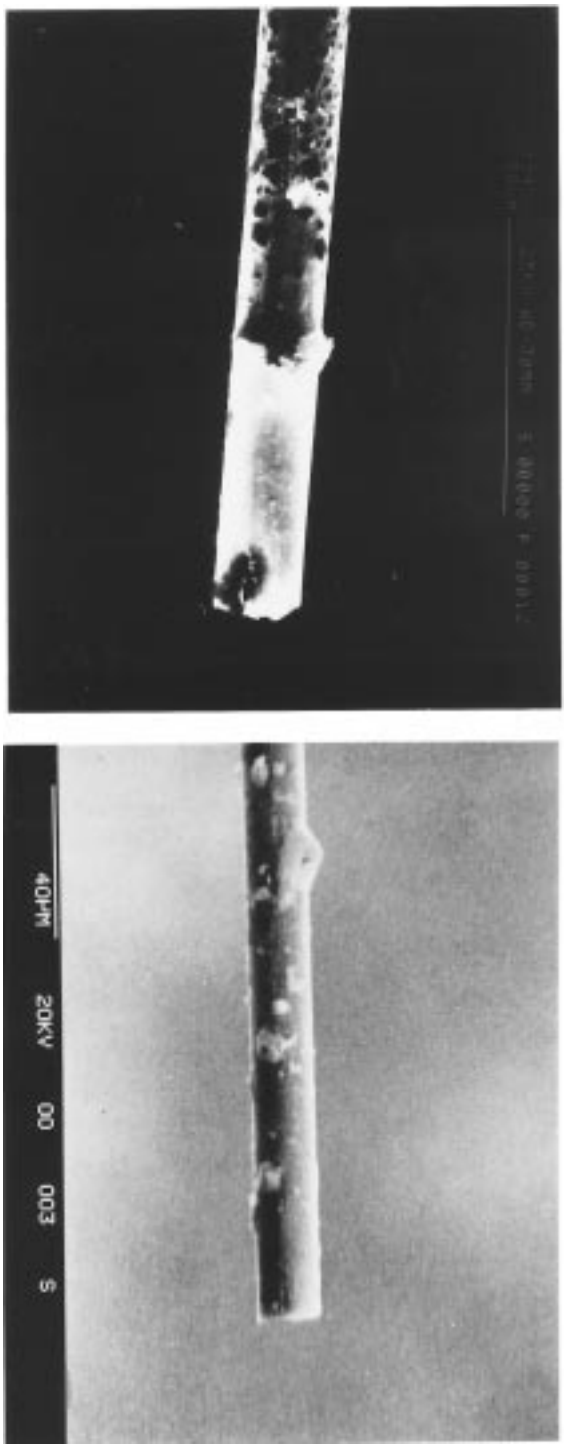

Figure 13. SEM views of the surface of polypyrrole-coated fibers, pretreated with (a, top) APS and (b, bottom) SP1.

point and the previous one are the expression of a strong adhesion between polypyrrole and glass, leading to a rupture occurring at the polypyrrole−matrix interface. Moreover the resin residue now appears as a part of the wetting cone. This indicates that the debonding results from the failure in tension of the matrix inside the wetting cone, the polypyrrole matrix interface being stronger than the matrix itself.

The τ_d value (65 MPa) deduced from pull-out experiments is a lower limit of the real adhesion stress, because it expresses only a stress state allowing tensile breaking of the matrix. Moreover the curve displayed in Figure 12b shows a significant dispersion, indicative of this failure mode.[34]

From all these results, it is clear that unlike the [glass/APS/polypyrrole] interface, the [glass/SP1/polypyrrole] one appears stronger than the [polypyrrole/resin] one, or than the bulk resin itself.

D.2. Tensile Pull-Off Tests. To state more precisely the benefit of using the specific silane SP1 for improving adhesion between glass (or more generally all silica-based materials) and polypyrrole, tensile pull tests were performed[35] on polypyrrole-coated silica plates, elaborated by using the same techniques as for the fibers (specific silanization, and vapor-phase deposition). For these tests, load is applied normal to the coating/substrate plane by means of a bonded stud. The measured breaking strength is related to the nature of the multilayered interphase inserted between the plate and the pull stud. Results of the tests demonstrates that (i) for the [APS/polypyrrole/resin] interphase, the polypyrrole layer separates from the plate, breaking strength being 29 MPa; (ii) for the [SP1/polypyrrole/resin] interphase, polypyrrole remains bound on the plate, breaking strength attaining now 71 MPa.

The latter value has to be compared to those relative to the interphases devoid of polypyrrole, viz., [APS (or SP1)/resin] or resin alone, all equal to 77 MPa, which corresponds also to the resistance of the bulk resin. On the contrary, for the interphase [polypyrrole/resin], without any silane, the strength is too low to be measured.

From all these measurements, it can be concluded that silanes improve adhesion between glass (or silica) and polypyrrole; but, while for SP1 this adhesion is high enough for overtaking the resin resistance itself, for APS, it is too low to prevent detachment of the conductive layer from the substrate.

III. Discussion and Conclusion

Two original features define the achieved improvements of materials described in the present paper: the surface pretreatment with new specific silanes as coupling agents on one hand, the vapor-phase polymerization of pyrrole on the other. Both of these characteristics succeeded not only in solving the problem of the adhesion mentioned at the beginning of this work, but also in leading to a polypyrrole layer with a conductivity higher than usual. It is worth noticing that both of these features can be included in a continuous, industrially attractive process for manufacturing conductive textile.[5]

The main goal addressed starting this work was to promote adherence of the polypyrrole deposit onto glass fibers. As attested by the results obtained by both mechanical measurements and SEM examination, a clear improvement of the polypyrrole layer adhesion is proved by comparing the behavior of the APS- and the SP1-treated fibers or plates. While the separation between the polypyrrole and the glass surface occurs at moderate stress with the APS-treated substrate, no separation at all is observed in the case of SP1 treatment, the rupture occurring in the resin, and the polypyrrole−fiber interface being in this case surpris-

(35) Le Bars, O. Thesis; Université Paris 6, Paris, 1997.

ingly more resistant that the usually strong resin−polypyrrole interface. This obviously proves the existence of a very strong SP1−polypyrrole interaction, perhaps the insertion of the pyrrole rings of SP1 in the first polypyrrole chains deposited. The present technique succeeded therefore in reaching its aim by improving considerably the adherence of polypyrrole on glass.

A surprising and also very interesting feature of the polypyrrole layer deposited from pyrrole vapor on SP1-coated fibers is that the intrinsic conductivity of the conducting polymer (about 100−200 S/cm) reaches a rather high value compared to the currently described polyprrole. This leads us to think that the above-mentioned characteristics (silane treatment, vapor-phase deposition) featuring the elaboration method of polypyrrole-coated glass surfaces are also able to induce some specific structural character, for instance a higher degree of order, at any level whatever, of the polypyrrole layer. This somewhat surprising and very interesting feature is now under investigation,[35−36] by working on silica plates, which were already mentioned in this paper for pull-off tests. The use of such specimens permits separating the conducting layer from the silica surface, allowing to study more easily the influence of the specific silane treatment on the morphology and structure of the polypyrrole coating in relation to its conductivity,[35] and to the evolution of the conductivity with aging.[28−37] The results of these studies will be related in detail in later papers.

IV. Experimental Part

A. Syntheses. *N-Glycidylpyrrole*: A reaction mixture formed from 200 g of sodium hydroxide, 8.4 g of tetrabutylammonium hydrogenosulfate, 200 mL of water, and 125 mL of epichlorohydrin is stirred very vigorously at room temperature in a 1 L reactor. Freshly distilled pyrrole (40 g, 0.6 mol) is added dropwise, with cooling in ice in order to keep the temperature of the mixture between 15 and 20 °C. The mixture is left stirring under a stream of nitrogen, the progress of the reaction is monitored by size-exclusion chromatography (SEC); the reaction is complete after 3 h. The aqueous phase is extracted with ether (3 × 100 mL). The organic phase is washed with aqueous NaCl solution until neutrality, dried over a molecular sieve, filtered, and distilled under vacuum. Yield 58 g (0.47 mol: 78%); purity > 98% by SEC; bp 80 °C/20 mmHg. ^{13}C NMR ($CDCl_3$,75 MHz) δ (ppm) 44.36, 50.51, 50.8, 108, 120.5.

3-{[3-(N-Pyrrole)-2-hydroxypropyl]amino}propyltriethoxysilane (SP1): 2.21 g (0.01 mol) of (3-aminopropyl)triethoxysilane (Aldrich) and 1.23 g (0.01 mol) of *N*-glycidylpyrrole are mixed in a suitably dried 50 mL round-bottomed flask. The mixture is set at room temperature, provided it is not lower than 25 °C. The progress of the reaction is monitored by NMR. In 1 or 2 days according to the temperature, all the *N*-glycidylpyrrole has been consumed, and SP1 is obtained. The compound is characterized by ^{1}H and ^{13}C NMR. Its purity is 85%, determined by NMR. The impureties are only of (3-aminopropyl)triethoxysilane and SP2. ^{13}C NMR ($CDCl_3$,75 MHz) δ (ppm) 4, 17.9, 22.7, 51.9, 53.5, 57.7, 58.1, 69.3, 108, 121. IR (KBr) ν(cm^{-1}):[38,39] ν(OH) 3400, ν(NH) 3700, ν(CH═*pyrrole*) 3123, 3100, νas(CH_3) 2974, νas(CH_2) 2927, νs(CH_3) 2885, νs(CH_2) 2870, ρ(CH_3) 1167, νas(Si−O−C) 1103, ν(C−O) 1080, νs (Si−O−C) 958.

3-{Bis[3-(N-pyrrole)-2-hydroxypropyl]amino}propyltriethoxysilane (SP2): 2.21 g (0.01 mol) of (3-aminopropyl)triethoxysilane and 2.46 g (0.02 mol) of *N*-glycidylpyrrole are mixed and reacted in the same way as before. The obtained SP2 is characterized by ^{1}H and ^{13}C NMR. Its purity is >95%, determined by NMR. ^{13}C NMR ($CDCl_3$,75 MHz): δ (ppm) 7.4, 18, 19.5, 53.3, 57.5, 58, 58.7, 68 and 69, 108, 121. IR (KBr) ν(cm^{-1}):[38,39] ν(OH) 3400, ν(CH═*pyrrole*) 3123, 3100, νas(CH_3) 2974, νas(CH_2) 2927, νs(CH_3) 2885, νs(CH_2) 2870, ρ(CH_3) 1167, νas(Si−O−C) 1103, ν(C−O) 1080, νs(Si−O−C) 958.

B. Spectroscopies. *Nuclear magnetic resonance (NMR) spectroscopy:* The ^{1}H and ^{29}Si nuclear magnetic resonance spectroscopies have been used in order to study hydrolysis and condensation reactions of silanes in solution. All spectra were recorded at 298 K on a Varian Unity 300 spectrometer operating at 299.95 MHz for ^{1}H and 59.59 MHz for ^{29}Si.

^{1}H π/2 pulse 11.5 ms; acquisition time 3 s; repetition time 20 s; scans number 2; spectral window 3200 Hz; for H_2O/acetic acid solutions, the water suppression was achieved by presaturation.

^{29}Si π/2 pulse19 ms; acquisition time 0.4 s; repetition time 30 s; scans number 2; spectral window 5460 Hz; insensitive nuclei enhanced by polarization transfer (INEPT) pulse sequence was used, the coupling constant J_{SiH} was 36 Hz.

Chemical shifts are referred to tetramethylsilane (TMS). For H_2O/acetic acid solutions no lock was used. For D_2O/acetic acid solutions, this former is used as internal lock.

Kinetics were performed in situ in the spectrometer. Times are referenced from the first recorded spectrum (experimental time).

Infrared spectroscopy: Infrared spectra were acquired using an IRTF 740 SX spectrometer (Nicolet) purged with dry air, equipped with a water-cooled Globar source, a pyroelectric DTGS detector (spectral window 0.25−500 mm), and a germanium-on-KBr beam splitter; the solutions were analyzed in a KRS-5 cell (thickness 13 mm); acquisition time 10 s (8 scans); resolution 4 cm^{-1}; repetition time 30 s.

Kinetics were performed in situ in the spectrometer.

Micro-Raman spectroscopy: Raman spectra have been obtained using XY Dilor equipment, consisting of an argon ion laser beam (457.9 nm) or a helium−neon laser beam (632.8 nm), focused on the specimen through a Nikon optical microscope that collects the reflected light and concentrates it to a premonochromator and finally to the spectrometer. High-quality (confocal) optics are provided to focus the incident laser beam to a 1 mm spot on the fiber and collect the 180° backscattered light. A Wright's Instruments cooled charged-coupled device (CCD) was employed as the detector for recording the Raman spectra. To limit local heating effects on the fiber, the incident power beam is limited to 150−500 mW and the fiber is continuously scanned over 80 mm around a central position.

X-ray photoelectron spectroscopy (XPS): The XPS measurements were made on a VG Escalab MkI spectrometer with a Al Kα X-ray source (1486.6 eV). The X-ray power supply was run at a power of 200 W (20 mA, 10 kV). The pressure in the analysis chamber was between 3×10^{-9} and 3×10^{-8} mbar. The analyzed area is equal to 0.4 cm^2. To compensate for surface charging effects, all XPS spectra were referenced to the C^{1s} neutral carbon peak at 285 eV. In spectral deconvolution, the full width at half-maximum of the Gaussian peaks was kept constant for the same component in all spectra. Surface elemental compositions were obtained from peak area ratios corrected with the following sensitivity factors 1, 3.1, 1.6, 2.5, and 1.2 for the C 1s, O 1s, N 1s, S 2p, and Si 2p bands.

C. Preparation of Solutions and Materials. Conditions for solubility tests: To 10 mL of bidistilled H_2O are added several concentrations of silanes (1−10% w/w). The pH is then adjusted by adding acetic acid in order to obtain solutions at pH 3.1, 3.5, 4.5, and 5.

Hydrolysis solutions: To 10 mL of bidistilled H_2O or D_2O (99.9%, Aldrich) are added several quantities of acetic acid (0.2, 0.4, 1, 1.5 mL) in order to obtain the concentrations 0.33, 0.65,

(36) Le Bars, O.; Attias, A. J., to be published.
(37) Sixou, B.; Vautrin, M.; Attias, A. J.; Travers, J. P. *Synth. Met.* **1997**, *84*, 835.
(38) Bellamy, J. P. *The Infrared Spectra of Complexes Molecules*, 3rd ed.; John Wiley and Sons: New York, 1975.
(39) Dirlikov, S.; Koenig, J. L. *App. Spectrosc.* **1979**, *33*, 551.

1.52, 2.17 mol L^{-1} respectively. Silanes are added at different concentrations (1−10% w/w) the resulting value of the pH being between 3 and 5. For example: the 0.29 M solution of SP1 in 10% (w/w) acetic acid in H_2O (1.52 mol L^{-1}) has pH 4.5.

Fibers: The fiber used was an E glass fiber produced by Vetrotex-Saint-Gobain (France), supplied as rovings, i.e., collections of untwisted parallel continuous glass filaments (800 filaments; glass fiber diameter 13 μm). The yarn is treated by Vetrotex with one of the following commercial silanes: (3-aminopropyl)triethoxysilane (APS), (glycidyloxypropyl)triethoxysilane (GPS), (methacryloyloxypropyl)triethoxysilane (MPS), or one of the specific silanes (SP1, SP2).

Polypyrrole-coated fibers: Vapor-phase coating is made by mounting the fiber yarn, a few centimeters long, on a little stand, and introducing it into a thin-layer chromatography developing tank, containing liquid pyrrole on the bottom and equipped with saturation pads.

Resistance measurements: The resistance of samples of coated yarn was measured with a simple laboratory ohmmeter, between two metal grips, 10 cm distant, used as electric contacts.

D. Adhesion Tests. *D.1. Pull-Out Tests.* Pull-out tests were carried out on E glass fiber monofilaments (diameter 13 mm) extracted from tows (800 fibers), silanized with one of the following silanes: SP1, APS, GPS, and MPS, and made according to section II.B; embedded lengh l_e range 50−600 mm; Ciba Geigy LY556 resin-27 wt % HT972 hardener was used (curing 2 h at 140 °C).

D.2. Tensile Pull-Off Tests. Tensile tests were carried out on silica plates coated with polypyrrole by the vapor-phase method after being pretreated by APS or SP1. Tensile load is applied normal to the coating/substrate plane until separation occurs.

Testing is accomplished by first attaching to the specimen an aluminum pull stud (diameter $\sim$ 3 mm) coated by a thin film made of an epoxy-hardener system (precoated studs furnished by Quad-Group). An adhesive joint between the polypyrrole layer and the stud is realized by curing the resin at 150 °C during 3 h. The test stud is then pulled by means of a special device (Sebastian II, Quad-Group). After separation, the specimen is examined in order to identify which interface has been broken. The bond strength is equal to the the breaking load divided by the area of bonding.

Acknowledgment. The authors would like to acknowledge Dr. J.-M. Bain from Vetrotex France S.A. for technical support and providing of E glass fibers rovings treated with commercial silanes on one hand and with silanes SP1 and SP2 on the other hand. The authors thank Dr. G. Désarmot (ONERA) for very helpful discussions concerning the pull-out tests and Dr. M. M. Chehimi (Institut de Topologie et de Dynamique des Surfaces, Université de Paris 7) for his help on obtention and interpretation of XPS spectra.

CM970466P